Lifetimes of Rydberg states in ZEKE experimensts III. Calculations of the DC electric lifetimes of NO.

Vrakking, M.J.J.

published in
Journal of Chemical Physics
1996

DOI (link to publisher)
10.1063/1.472592

document version
Publisher's PDF, also known as Version of record

Lifetimes of Rydberg states in ZEKE experiments. III. Calculations of the dc electric field dependence of predissociation lifetimes of NO

Marc J. J. Vrakking
Laser Centrum Vrije Universiteit, Faculteit der Scheikunde, De Boelelaan 1083, 1081 HV Amsterdam, The Netherlands

(Received 21 June 1996; accepted 23 July 1996)

Results are presented of calculations on the experimentally observed lifetime enhancement of high principal quantum number $nf(N^+=2)$ and $np(N^+=0)$ Rydberg states of the NO molecule in small dc electric fields. A Hund's case (d) molecular Hamiltonian is introduced, which describes intramolecular interactions between low angular momentum Rydberg states as a result of core penetration and l mixing caused by the electric field. Eigenstates of the molecule in the electric field are obtained by diagonalization of the Hamiltonian and an effective decay time is determined which describes the multiexponential decay of the superposition of (Stark) states which is excited experimentally. The calculations reproduce the striking onset of the lifetime enhancement of the $np(N^+=0)$ series, which was observed experimentally. Both for the $nf(N^+=2)$ and $np(N^+=0)$ Rydberg series, core penetration by low-l states leads to extensive interseries coupling for several values of the principal quantum number. © *1996 American Institute of Physics.*
[S0021-9606(96)00541-7]

I. INTRODUCTION

In recent years there has been considerable interest in the decay dynamics of high principal quantum number atomic and molecular Rydberg states in the context of the remarkable success of the technique of zero-electron kinetic energy photoelectron spectroscopy (ZEKE-PES).[1,2] As has been abundantly documented, in ZEKE experiments a breakdown of the n^3 scaling law for the lifetime is frequently observed, where the lifetimes of the detected Rydberg states are several orders of magnitude longer than anticipated based on extrapolation of the lifetimes of low-n Rydberg states.[3] These observations have led to considerable experimental and theoretical activity, and theories explaining the lifetime enhancements in terms of intramolecular phenomena, intermolecular interactions and external field effects have been proposed and subjected to experimental verification.[4–12] Here, we particularly consider the angular momentum mixing model first proposed by Chupka,[6] which was based on the work by Bordas *et al.*[13] Chupka suggested that the long lifetimes observed in ZEKE experiments could possibly be explained by the fact that under typical ZEKE conditions dc stray electric fields cause a mixing of the orbital angular momentum states of the Rydberg electron. This causes the optically excited low-l orbital to be mixed with high-l nonpenetrating orbitals. Unlike low-l orbitals, these orbitals interact only weakly with the ionic core, and therefore have low rates for decay processes such as autoionization, predissociation and fluorescence. If dc electric fields lead to a dilution of the low-l character of the wave function, a significant Rydberg lifetime enhancement is expected.

In order to investigate the model by Chupka, we experimentally studied the lifetimes of high-n ($n=40-120$) p- and f-orbital Rydberg states of the NO molecule.[11(a),11(b)] Individual high principal quantum number p- and f-orbital Rydberg states were prepared using a tunable near transform-limited pulsed dye laser, and lifetimes were determined using delayed pulsed field ionization. The outcome of these experiments provided strong support for the model proposed by Chupka. The lifetimes of the high-n Rydberg states could be significantly enhanced by the application of a small dc electric field which mixes the low-l state which is optically excited with a nearby Stark manifold. Specifically, for a dc electric field estimated at 25 mV/cm f-orbital Rydberg states converging on $N^+=1$ and 2 exhibited an approximately eightfold lifetime enhancement near $n=65$, whereas the lifetimes of p-orbital Rydberg states converging on $N^+=0$ and 1 went up sharply by nearly two orders of magnitude around $n=115$. Surprisingly, for the p-orbital Rydberg series the transition from ''short'' to ''long'' lifetimes took place for a unit change of the principal quantum number.

To illustrate the suddenness of the lifetime enhancement, experimental pulsed field time delay scans are reproduced in Fig. 1 for the 115p and 116p states converging on $N^+=0$, along with a relevant portion of the Rydberg excitation spectrum. The excitation spectrum [Fig. 1(a)] was obtained by measuring the total NO^+ ion yield as a function of the laser frequency, at a fixed time delay of about 10 ns between the laser excitation and the pulsed field ionization and extraction. In the spectrum Rydberg progressions corresponding to $np(N^+=0)$ and $nf(N^+=2)$ are observed. There is no indication in the spectrum of a qualitative difference between $np(N^+=0)$ levels with $n\leqslant 115$ and levels with $n\geqslant 116$. Time delay scans were carried out where the NO^+ signal was measured as a function of the pulsed field ionization time delay. They show significant differences between the $115p(N^+=0)$ and $116p(N^+=0)$ states. In the middle frame [Fig. 1(b)] the pulsed field ionization signal following preparation of the $115p(N^+=0)$ and $116p(N^+=0)$ states is shown on a short time scale, where the $115p(N^+=0)$ state is seen to decay with a time constant of 7.1 ± 1.6 ns, whereas

 0021-9606/96/105(17)/7336/12/$10.00

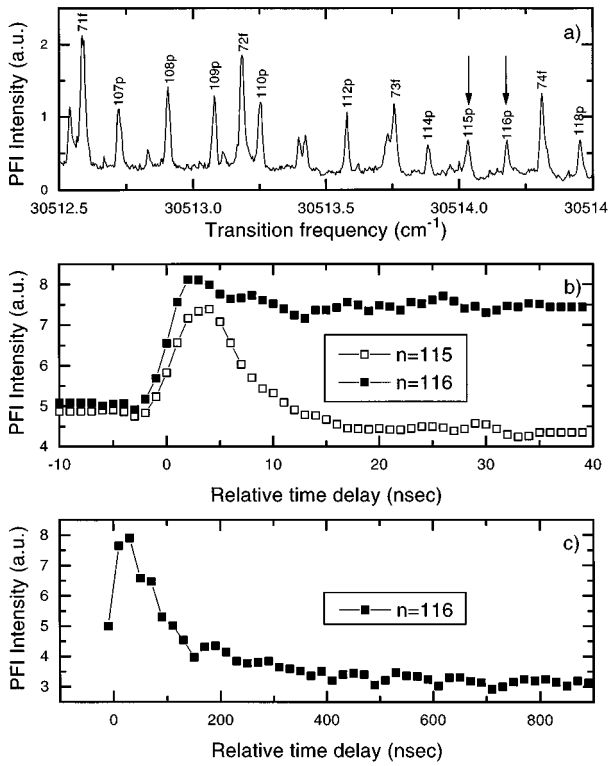

FIG. 1. (a) Experimental pulsed field ionization (PFI) excitation spectrum of the NO molecule starting from the $A\ ^2\Sigma^+(N_A=0,\ J_A=1/2)$ state, showing resolved Rydberg progressions $np(N^+=0)$ and $nf(N^+=2)$; (b) and (c) Experimental PFI time delay scans, showing the detected NO^+ signal as a function of the time delay between the excitation laser, which is tuned to a peak in the excitation spectrum corresponding to the $115p(N^+=0)$ or $116p(N^+=0)$ level. The decay curve for the $115p(N^+=0)$ level (b) fits with a decay time $\tau=7.1\pm1.6$ ns, whereas the decay curve for the $116p(N^+=0)$ level (c) fits with a decay time $\tau=114\pm27$ ns. See text and Refs. 11(a) and 11(b) for details.

the $116p(N^+=0)$ state shows hardly any decay. As shown in the lower frame [Fig. 1(c)], the $116p(N^+=0)$ state decays on a significantly slower time scale [notice the difference in the horizontal scales between Figs. 1(b) and 1(c)!], which is characterized by a decay time of 114 ± 27 ns. Experimentally, all states with $n<115$ undergo a rapid decay similar to $n=115$, whereas states with $n>116$ decay on a slow time scale, like $n=116$. Thus, in going from $115p$ to $116p$ the $np(N^+=0)$ series has undergone a dramatic lifetime enhancement of more than one order of magnitude.

Our experiments on NO led to theoretical work by Bixon and Jortner,[14] who extended the effective Hamiltonian formalizm which had already been used successfully to explain the lifetimes of autoionizing Rydberg states of Ar and DABCO.[8] In their calculation, Bixon and Jortner considered the l mixing caused by (i) long range intramolecular Rydberg electron–core dipole interactions and (ii) the external dc electric field. Except for a few accidental near degeneracies between low-l states they found that the electron–core dipole interactions were negligible. Therefore, the dynamics of the high-n Rydberg states of NO is practically unaffected by the long range intramolecular Rydberg electron–core dipole coupling, and dominated by Stark coupling.

Bixon and Jortner successfully calculated the lifetime enhancement of the f-orbital Rydberg series, while obtaining semiquantitative agreement for the lifetime enhancement of the p-orbital Rydberg series, where, in their calculation, the l mixing takes place over a range of $\Delta n\approx20$. They elegantly drew the analogy between l mixing induced by a dc electric field and intramolecular dynamics in isolated molecules. The low-l states act as doorway states for the optical excitation, and are coupled to available decay channels like predissociation and autoionization. The electric field provides a coupling of the doorway and decay states to a ''bath'' of high-l states, diluting the low-l character among a large number of eigenstates, in much the same way that in intramolecular vibrational relaxation the oscillator strength of a bright state is diluted among a large number of states.

Over the last two decades, the formalizm of multichannel quantum defect theory (MQDT) has been extremely successful in describing the spectroscopy and dynamics of highly excited Rydberg states.[15,16] At the core of MQDT lies the recognition that over its trajectory a Rydberg electron with low orbital angular momentum spends time in two physically distinct regions. When the electron is near the ionic core, it moves at a very high velocity and adjusts to the motions of the core (Born–Oppenheimer regime). The orbital angular momentum of the Rydberg electron is strongly coupled to the internuclear axis with a projection Λ, and combines with the rotational angular momentum R to yield the total angular momentum excluding spin $\mathbf{N}=\mathbf{L}+\mathbf{R}\cdot\mathbf{N}$ then combines with the electron spin $\mathbf{S}$ to given $\mathbf{J}$ [Hund's case (b)]. On the other hand, when the electron is far away from the ionic core, it moves very slowly, and no longer adapts to the motions of the core. The orbital angular momentum of the electron is no longer coupled to the internuclear axis, and the electron is best described in a space-fixed, rather than a molecule-fixed, frame. The angular momentum of the rotational motion, now called $\mathbf{N}^+$, is well-defined and combines with the angular momentum of the electron to give the total angular momentum excluding spin $\mathbf{N}=\mathbf{l}+\mathbf{N}^+$ [Hund's case (d)]. One of the central concepts of MQDT is the frame transformation which connects the states which are appropriate for a description of the molecule in the space-fixed frame of Hund's case (d) to those appropriate in the molecule-fixed frame of Hund's case (b).

In MQDT the electron wave function at long range is written as a linear combination of the two Coulomb functions f and g, which are analytical solutions for the motion of an electron moving under the influence of a Coulomb potential. The interactions of the electron with the ionic core are given by a number of quantum defects which describe the extent of mixing of the functions f and g induced by the core, for various core and electron angular momentum configurations, referred to as ''channels'' in MQDT. Since the electron is strongly accelerated towards the ionic core, the quantum defects depend only very weakly on the initial energy of the Rydberg electron. Bound Rydberg levels are found by requiring that the electron wave function vanishes for $r\Rightarrow\infty$, and in this fashion the quantum defects determine the Rydberg energy level structure.

Incorporation of the effects of an electric field in MQDT, as carried out by a number of researchers,[17–20] requires a description of the molecule that distinguishes three rather than two regimes for the electron. First of all, as before, there exists a core region, where the molecular is described in Hund's case (b). Secondly, there is a Coulombic region, where the molecule is described in Hund's case (d). And finally, there exists an asymptotic region where the interaction of the electron with the external electric field exceeds the Coulomb interaction with the ionic core, and where a description in terms of parabolic states becomes appropriate. This requires the use of two successive frame transformations.

While formally an MQDT approach is preferable in that it provides a unified treatment of the Rydberg dynamics at all values of the principal quantum number, we present in this paper results of calculations on the l mixing caused by a dc electric field using a perturbative approach. The results of a field-free MQDT treatment by Fredin and co-workers[21,22] were applied in a perturbative treatment using a Hund's case (d) basis set, making use of the prescription of Jungen to evaluate matrix elements which describe the coupling between case (d) basis states arising from short range electron–core interactions which are given by Hund's case (b) quantum defects.[23,24] Actually, the influence of a dc field on the excitation spectrum of intermediate-n Rydberg states of NO was noted by Fredin *et al.* who carried out their experiments in a dc field of 9 V/cm and who included a semiquantitative treatment of Stark mixing among s, p, and d orbitals in their paper.

In Hund's case (d) the coupling matrix elements that result from the interaction of the Rydberg electron with an electric field can readily be evaluated using standard angular momentum algebra. Diagonalization of the molecular Hamiltonian provides the composition of the Stark eigenstates in terms of the Hund's case (d) basis states, and lifetimes of these states are then evaluated assuming appropriate decay widths for the individual case (d) states.[25] This method differs from the method by Bixon and Jortner, who directly incorporate the decay as an imaginary diagonal matrix element in an effective Hamiltonian and diagonalize complex matrices. On the other hand, in our approach short range electron–core interactions leading to the coupling of core rotational states and the mixing of low-l Rydberg orbitals are taken into account, as exemplified by the fact that our calculation satisfactorily reproduces rotational perturbations in the field-free Rydberg spectrum of NO, as calculated and measured by Fredin *et al.*[21] Our work was motivated by the hope that a perturbative approach based on the results of MQDT (rather than a formal MQDT approach itself) may on the one hand provide an accurate description of the dc electric field lifetime enhancement of the high-n Rydberg states of NO, while, on the other hand, providing detailed insight into the individual role of a number of molecular interactions. We note that a similar approach was taken by Bordas and Helm, in their interpretation of the Stark spectrum of the H_3 molecule.[26]

In the current paper, we describe our approach and present results of calculations on the dc electric field induced lifetime enhancement of $nf(N^+=2)$ and $np(N^+=0)$ Rydberg series, where we emphasize the role of short range interactions. These short range interactions are represented by a finite number of quantum defects which describe different electronic (core+electron) configurations, as well as mixing that may occur between some of these configurations.

II. DESCRIPTION OF THE CASE (d) HAMILTONIAN

As described in the Introduction, our approach to study the electric field dependence of the lifetimes of the NO Rydberg states is based on a perturbative treatment, where the eigenstates in the field are determined through diagonalization of the molecular Hamiltonian. In setting up the Hamiltonian, a distinction was made between the penetrating and nonpenetrating orbitals. For orbitals with angular momentum $l \leqslant 2$ the electron interacts strongly with the ionic core, and for these core-penetrating orbitals the matrix elements were derived from a limited number of Hund's case (b) quantum defects. For $l \geqslant 3$ coupling between different Rydberg orbitals due to core penetration was ignored, and the zero-order energies were determined using the long range force model.[27,28]

We will now discuss the different terms which appear in the molecular Hamiltonian. First the electronic Hamiltonian will be introduced for both the penetrating and the nonpenetrating orbitals, followed by a discussion of the rotational Hamiltonian and finally the perturbation due to a dc electric field. The Hamiltonian is schematically represented in Fig. 2, where for a given value of the principal quantum number, states with orbital angular momentum up to $l=2$ and with core rotational angular momentum up to $N^+=2$ are shown, as well as the couplings which occur among these states within our model.

In writing down the Hamiltonian, a choice needs to be made between working with a Hund's case (b) or a Hund's case (d) basis set. In principle, the advantage of using a Hund's case (b) basis set is that the electronic part of the Hamiltonian is diagonal in Hund's case (b), except for a few terms which describe the mixing of $s\sigma$ and $d\sigma$ configurations. The nonzero elements of the case (b) electronic Hamiltonian are given by[23]

$$H^{(b)}_{\text{electronic}}[lN\Lambda, lN\Lambda] = -\mu_{l\Lambda}/\nu^3, \tag{1}$$

where $\mu_{l\Lambda}$ is a quantum defect and ν is the effective principal quantum number of the state under consideration.

The advantage of a near-diagonal electronic Hamiltonian in Hund's case (b) is negated, however, by the fact that in Hund's case (b) the rotational coupling terms are complicated, whereas in Hund's case (d) the rotational part of the Hamiltonian is diagonal. The high-n NO Rydberg levels are most conveniently described by specifying the orbital angular momentum l and the convergence limit given by the core rotational quantum number N^+, and therefore, we proceed by writing down the Hamiltonian in the case (d) basis set. For the electronic part of the Hamiltonian, this requires that

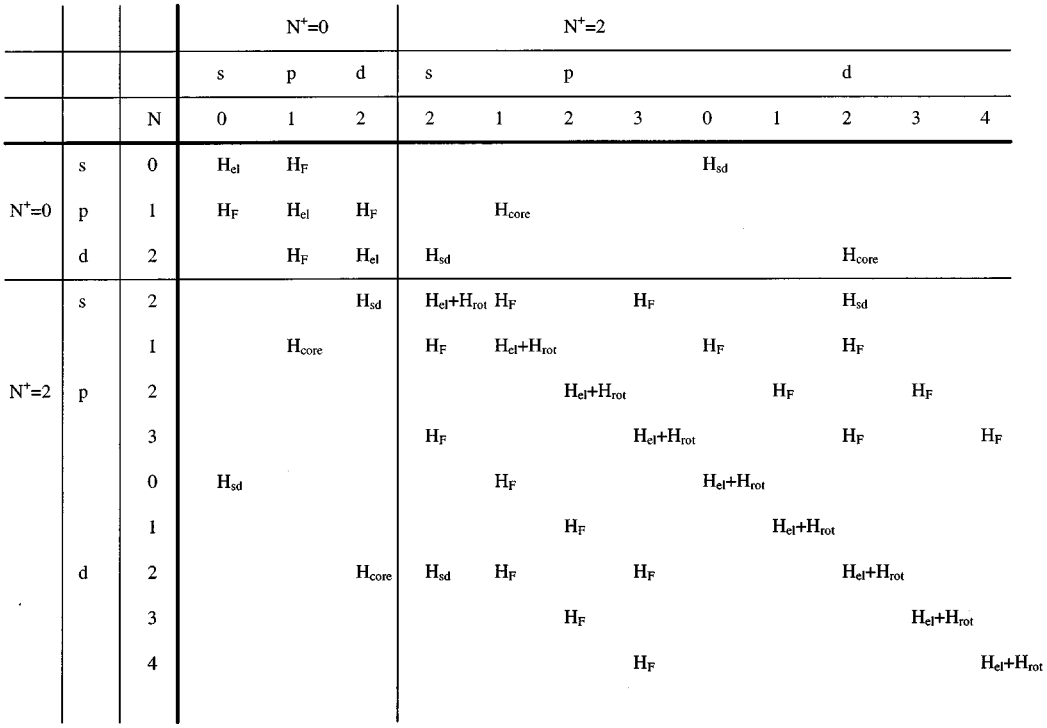

FIG. 2. Schematic case (d) Hamiltonian, showing the terms which are included in the calculations discussed in this paper. $H_{\rm el}$ are the diagonal terms of the electronic Hamiltonian, which are obtained by a frame transformation involving the Hund's case (b) quantum defects for $l \leqslant 2$, and from the long range force model for $l \geqslant 3$. $H_{\rm core}$ are matrix elements obtained through the same frame transformation, which, for given $l=0-2$, couple different case (d) rotational states. H_{sd} denote matrix elements between s- and d-orbital case (d) states, which are obtained from the case (b) quantum defects and are a result of the mixing of the $s\sigma/d\sigma$ core configurations. $H_{\rm rot}$ represents the rotational Hamiltonian, which is diagonal in Hund's case (d). Finally, H_F represent the terms describing the couplings due to the dc electric field. This schematic case (d) Hamiltonian only shows Rydberg states for one value of the principal quantum number, with $l \leqslant 2$ and $N^+ \leqslant 2$. In the actual calculations reported in this paper, within a prescribed energy range all Rydberg states with $N^+ \leqslant 4$ were used (i.e., including several values of the principal quantum number and including all $l \leqslant n-1$), leading to a Hamiltonian containing up to 1400 case (d) basis states.

the electronic Hamiltonian in the case (b) basis set is transformed to the case (d) basis set using a frame transformation,

$$H^{(d)}_{\rm electronic}[lNN^+,l'NN^{+\prime}] = \Sigma_{\Lambda\Lambda'} A_{N^+\Lambda} H^{(b)}_{\rm electronic}[lN\Lambda,l'N\Lambda'] A_{N^{+\prime}\Lambda'}, \quad (2)$$

where $A_{N^+\Lambda}$ is given by[16]

$$A_{N^+\Lambda} = (-1)^{l+\Lambda-N^+} \begin{pmatrix} l & N & N^+ \\ -\Lambda & \Lambda & 0 \end{pmatrix} \times (2N^+ + 1)^{1/2} [2/(1+\delta_{\Lambda 0})]^{1/2}. \quad (3)$$

The transformation given by Eq. (2) gives the relation between the case (b) and case (d) quantum defects, and thereby provides the diagonal terms of the electronic case (d) Hamiltonian. These terms are designated $H_{\rm el}$ in the schematic case (d) Hamiltonian shown in Fig. 2. Furthermore, Eq. (2) also shows how Rydberg series converging on *different* core rotational states are coupled. As the electron approaches the ionic core, it reaches the Born–Oppenheimer region where the case (d) coupling scheme no longer applies and where the molecule is best described in Hund's case (b). The orbital angular momentum of the electron couples to the internuclear axis with a projection Λ, and the core rotational quantum number N^+ loses its meaning. Subsequently, as the electron reemerges from the Born–Oppenheimer region, a case (d) description becomes appropriate once again, but now the core rotational state may no longer be the same one as prior to the electron–core collision. By this mechanism states with the same electron orbital angular momentum l and total angular momentum excluding spin N but *different* core rotational states N^+ are coupled, as shown in the schematic case (d) Hamiltonian in Fig. 2, where these coupling matrix elements are represented by $H_{\rm core}$.

As mentioned in the introduction to this paragraph, the electronic part of the case (b) Hamiltonian is assumed to be diagonal, except for a few terms which describe the mixing of $s\sigma$ and $d\sigma$ configurations.[29] As a result of the $s\sigma/d\sigma$ mixing, case (b) matrix elements involving these configurations are modified to[21]

$$H^{(b)}_{\rm electronic}[sN0,sN0] = -(\mu_{s\sigma} \cos^2\theta + \mu_{d\sigma} \sin^2\theta)/\nu_{s\sigma}^{3/2}\nu_{d\sigma}^{3/2}, \quad (4)$$

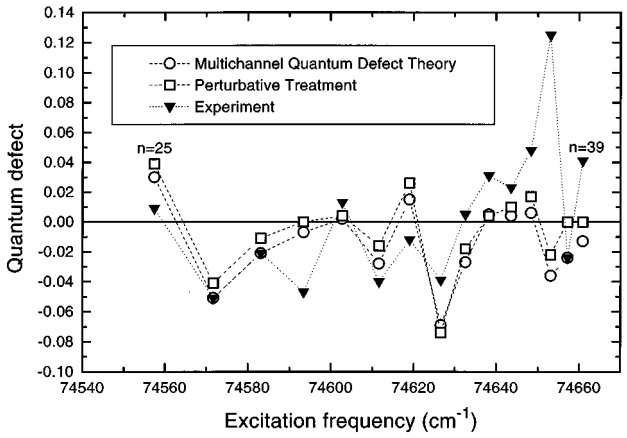

FIG. 3. Comparison between quantum defects of the $ns(N^+=2)$ Rydberg series of NO calculated using the method in this paper (□) and results of the MQDT analysis by Fredin *et al.* (Ref. 21) (○). This Rydberg series is perturbed by interactions with *s*- and *d*-Rydberg series converging on $N^+=0-4$, which are represented by $H_{\rm core}$ and H_{sd} in the schematic molecular Hamiltonian (Fig. 2). Also shown are the experimental results of Fredin *et al.* (Ref. 21) (▼).

$$H^{(b)}_{\rm electronic}[dN0,dN0] = -(\mu_{s\sigma}\sin^2\theta+\mu_{d\sigma}\cos^2\theta)/\nu_{s\sigma}^{3/2}\nu_{d\sigma}^{3/2}, \quad (5)$$

$$H^{(b)}_{\rm electronic}[sN0,dN0] = -\tfrac{1}{2}\sin 2\theta(\mu_{s\sigma}-\mu_{d\sigma})/\nu_{s\sigma}^{3/2}\nu_{d\sigma}^{3/2}. \quad (6)$$

For NO the $s\sigma/d\sigma$ mixing is described by a mixing angle θ of $-38.7°$. Like the diagonal case (b) matrix elements [Eq. (1)] the matrix elements of Eqs. (4)–(6) are transformed to matrix elements in case (d) using the frame transformation of Eqs. (2) and (3). Due to the $s\sigma/d\sigma$ mixing *s* and *d* orbitals converging on different core rotational states N^+ are coupled in the case (d) Hamiltonian, subject to the condition that the total angular momentum excluding spin *N* is conserved. In the schematic case (d) Hamiltonian in Fig. 2 these matrix elements are represented by H_{sd}.

In our discussion of the electric field dependence of the lifetimes of the Rydberg states of NO we want to pay special attention to the role of the short range matrix elements $H_{\rm core}$ and H_{sd}, which were not yet included in the treatment by Bixon and Jortner.[14] These couplings are of significant importance in determining the field-free energy levels of the NO molecule. To illustrate this and to test the quality of our perturbative approach we present in Fig. 3 a calculation of perturbations which occur for intermediate $n(n=25-39)$ in the quantum defects of the *s*-orbital Rydberg series converging on $NO^+(N^+=2)$. Quantum defects for this Rydberg series were determined both experimentally and theoretically (using MQDT) by Fredin *et al.*[21] In our calculation we used the case (b) *s*- and *d*-orbital quantum defects and the $s\sigma/d\sigma$ mixing angle given by Fredin *et al.* and included rotational levels of the NO^+ ion up to $N^+=4$. The results of the calculation are shown in Fig. 3, where quantum defects of selected lines containing a significant $s(N^+=2)$ component are compared to the quantum defects calculated by Fredin *et al.*[21] The agreement between the perturbative approach and the MQDT calculation is quite satisfactory. In fact, the deviations between the two theories are significantly smaller than the differences between either theory and the experimental results of Fredin *et al.* which are also shown in Fig. 3.

It is anticipated that the coupling matrix elements $H_{\rm core}$ and H_{sd} could have a significant role when the application of a dc electric field is considered. An example in the literature is the Stark spectrum of H_2, where matrix elements $H_{\rm core}$ are responsible for significant perturbations between two *p*-orbital Rydberg series converging on $N^+=0$ and 2, leading to major intensity variations in the experimental Stark manifold that is obtained when these *p* orbitals are mixed with the high-*l* manifold.[30] An example of the role of H_{sd} was seen in our earlier work on the pulsed field ionization of Xe atom in a electric field.[11(c)] In these experiments pulsed field ionization of *s*- and *d*-orbital Rydberg series converging on the spin–orbit excited $^2P_{1/2}$ state of Xe^+ was studied. These Rydberg series have reduced quantum defects of 0.01 and 0.30, respectively. Based on the sequential $(\Delta l=\pm 1)$ nature of the couplings induced by the electric field, one would anticipate that the onset for mixing of the *s* orbital with the nearby high-*l* manifold could only occur *after* the field conditions for mixing of the *d* orbital with the high-*l* manifold have been met. Experimentally, however, the onset for mixing of the *s* series with the high-*l* manifold occurred at a significantly lower field than for the *d* series. Calculations using the approach outlined in this section illustrate that this behavior can be explained by $s\sigma/d\sigma$ mixing,[31] which for Xe is known to occur with a mixing angle of 0.1 rad.[32]

As mentioned in the introduction to this section, for the nonpenetrating orbitals the diagonal terms of the electronic Hamiltonian were calculated using the long range force model.[27,28] Following the treatment of Jungen and Miescher,[28] the energy of interaction of a nonpenetrating Rydberg electron with the ionic core is given by

$$\Delta E_{n,l,\mathscr{S}} = -(1/4)Q_{zz}\langle 1/r^3\rangle_{n,l}\langle 3\cos^2\theta-1\rangle_{l,\mathscr{S}}+\tfrac{1}{2}\langle 1/r^4\rangle_{n,l} \times\langle \alpha+(1/6)(\alpha_{\rm perp}-\alpha_{\rm par})(3\cos^2\theta-1)\rangle_{l,\mathscr{S}}, \quad (7)$$

where

$$\langle 3\cos^2\theta-1\rangle_{l,\mathscr{S}} = -2[3\mathscr{S}^2-l(l+1)]/[(2l-1)(2l+3)], \quad (8)$$

and $\mathscr{S}=N-N^+$.[33] $\Delta E_{n,l,\mathscr{S}}$ is the energy by which a case (d) level $(n,l,\mathscr{S})$ lies below the hydrogenic term $-1/2n^2$. In Eq. (7) Q_{zz} is the quadrupole moment of the electronic charge distribution of the ionic core with respect to the molecular axis, and $\alpha=(2\alpha_{\rm perp}+\alpha_{\rm par})/3$ is the spherical polarizability of the core, where $2\alpha_{\rm perp}$ and $\alpha_{\rm par}$ are the polarizabilities of the core parallel and perpendicular to the molecular axis, respectively. θ is the polar angle of the electron. The energy of interaction can be evaluated using tabulated radial integrals $\langle 1/r^3\rangle_{n,l}$ and $\langle 1/r^4\rangle_{n,l}$.[34] Using Eqs. (7) and (8) Jungen and Miescher interpreted the structure of the *nf* complexes of NO, resulting in the determination of $\alpha=7.64$ a.u. and (assuming $\alpha_{\rm perp}-\alpha_{\rm par}=\alpha/3$) of $Q_{zz}=0.59$ a.u. Using these parameters an asymptotic high-*n* quantum defect of 0.0141 is

calculated for both the ($N^+=2$, $N=1$, $\mathscr{S}=-1$) and ($N^+=1$, $N=2$, $\mathscr{S}=1$) f-orbital Rydberg series for which the lifetime experiments were carried out, which compares reasonably well with the experimental values of 0.0101 and 0.0168, respectively.

The rotational part of the Hamiltonian is diagonal in the case (d) basis set and the nonzero matrix elements are simply given by

$$H^{(d)}_{\text{rotational}}[lNN^+,lNN^+]=B_{\text{rot}}N^+(N^++1), \tag{9}$$

where B_{rot} is the rotational constant of the NO^+ core. In the schematic case (d) Hamiltonian shown in Fig. 2, the rotational matrix elements are represented by H_{rot}. In our calculations only Rydberg states converging on the ground vibrational state of the NO molecule are considered.

The case (d) Hamiltonian described thus far provides a field-free description of the molecule, where the level structure is determined by the case (b) quantum defects, the ionic rotational constant and the $s\sigma/d\sigma$ mixing angle. Having established, by comparison with the results of MQDT, that this Hamiltonian gives a good description of the level structure of the NO molecule under field-free conditions, we finally need to consider the influence of an electric field on the Rydberg states. The electric field couples orbital angular momentum states of the electron subject to the selection rules $\Delta l=\pm 1$, $\Delta N=0,\pm 1$ and $\Delta N^+=0$. Using the Wigner–Eckart theorem[35] the matrix elements can be evaluated as

$$\begin{aligned}H^{(d)}_{\text{field}}[lNN^+,l'N'N^+]&=-eF\langle \nu lN^+NM_N|z|\nu' l'N^+N'M'_N\rangle\\&=-eF(-1)^{N-M_N+l+N^++N'+1}[(2N+1)(2N'+1)]^{1/2}\\&\times\begin{pmatrix} N & 1 & N' \\ -M_N & 0 & M_{N'}\end{pmatrix}\begin{Bmatrix} l & N & N^+ \\ N' & l' & 1\end{Bmatrix}\langle \nu l\|r\|\nu' l'\rangle,\end{aligned} \tag{10}$$

where

$$\langle \nu l\|r\|\nu' l'\rangle=\begin{cases}-(l+1)^{1/2}\langle \nu l|r|\nu' l+1\rangle & l'=l+1\\ l^{1/2}\langle \nu l|r|\nu' l-1\rangle & l'=l-1.\end{cases} \tag{11}$$

The radial integrals were evaluated using the results of Edmonds *et al.*[36] where

$$\langle \nu l|r|\nu' l'\rangle=\{3/2\ \nu_c^2[1-(l_c/\nu_c)^2]^{1/2}\}\Sigma_{p=0,3}\gamma^p g_p(s), \tag{12}$$

with $\gamma=\Delta l(l_c/\nu_c)$, $s=\nu-\nu'$, $l_c=\max(l,l')$, $\Delta l=l'-l$, and $\nu_c=2/(1/\nu+1/\nu')$. The function $g_p(s)$ ($p=0,3$) is tabulated in Ref. 36.

To summarize, in the case (d) Hamiltonian shown in Fig. 2 we employ the following terms: (i) diagonal terms of the electronic and rotational Hamiltonian, (ii) coupling terms arising from the case (b) quantum defects, and (iii) coupling terms as a result of the dc electric field. The coupling terms arising from the case (b) quantum defects are terms which couple levels with the same N, and the same or different l and N^+. For all of these terms the mixing of core rotational states is subject to $\Delta N^+=$even. Combined with the selection rule for the coupling by the dc electric field ($\Delta N^+=0$), the case (d) basis states separate into two groups, distinguished by N^+ being even or odd, which only interact among themselves. In what follows we will be concerned with the mixing of the $np(N^+=0)$ and $nf(N^+=2)$ series, which were studied experimentally through excitation from the $A\ ^2\Sigma^+(N_A=0, J_A=1/2)$ intermediate state. Therefore, in our calculations only rotational states with $N^+=$even were included.

We emphasize that at the current level of our calculations the long range Rydberg electron-core dipole interaction, which was studied by Bixon and Jortner, is *not* included. Bixon and Jortner demonstrated that, *except* for a few isolated occurrences such as the lifetime enhancement of the $92p(N^+=0)$ and $95p(N^+=0)$ Rydberg states, the role of the long range Rydberg electron–core dipole interaction, which leads to a coupling of odd and even rotational states ($\Delta N^+=\pm 1$), is unimportant. As a result the lifetime enhancement of the $92p(N^+=0)$ and $95p(N^+=0)$ Rydberg states, which was observed experimentally well before mixing with the nearby $N^+=0$ high-l manifold was anticipated, is not reproduced in our calculation. The lifetime enhancement of the $92p(N^+=0)$ and $95p(N^+=0)$ Rydberg states is an example of the interplay between electric field effects and intramolecular couplings: the long range Rydberg electron–core dipole interaction provides a coupling of the $92p(N^+=0)$ and $95p(N^+=0)$ states to the $80d(N^+=1)$ and $82d(N^+=1)$ states, respectively, which subsequently undergo lifetime enhancement by coupling to nearby $n=80$ and $n=82$ ($N^+=1$) Stark manifolds as a result of the presence of a dc electric field.[14] A similar interplay between dc electric field interactions and Rydberg electron–core quadrupole interactions has been invoked by Merkt *et al.*[7(a)] in order to explain the large changes in rotational angular momentum observed in a number of ZEKE experiments. We would now anticipate that a similar interplay may exist between electric field interactions and short range interactions among the core-penetrating low-l states.

III. PROCEDURE TO CALCULATE THE EXPERIMENTALLY MEASURED LIFETIME

In our pulsed field ionization experiments np and nf Rydberg levels were excited using two-color double-

resonant excitation, employing the $A\ ^2\Sigma^+$ ($N_A=0$ or 1) state as resonant intermediate.[11(a),11(b)] In order to measure the lifetime at observed resonances, a near transform-limited ns pulsed dye laser was positioned at frequencies where peaks appeared in an excitation spectrum which was measured using the shortest possible experimental pulsed field time delay ($\sim$10 ns). Effective lifetimes were determined by measuring the pulsed field ionization signal as a function of the pulsed field time delay. The lifetimes quoted in Refs. 11(a) and 11(b) were determined by fitting the measured time delay curves to a sum of a single-exponential decay and a constant background, which is due to ionization of Rydberg states by the excitation lasers. In this section we will discuss how these experiments are simulated on the computer, and how effective lifetimes are determined from the calculated composition of the Stark states.

Following diagonalization of the molecular Hamiltonian the eigenenergies of the Stark states are obtained, as well as expressions for the eigenvectors of the Stark states in terms of the case (d) basis functions

$$|i\rangle_{\text{Stark}}=\Sigma_\alpha A_{i\alpha}|\alpha\rangle_{\text{case }(d)}. \tag{13}$$

Equation (13) shows how, as a result of the mixing induced by the electric field and the short range interactions, the wave function amplitude of a particular doorway state $|\alpha_0\rangle_{\text{case }(d)}$ is spread over the manifold of Stark states $|i\rangle_{\text{Stark}}$. As a result, a similar spreading occurs for other observables associated with the doorway state, such as the absorption cross section and the decay rate. The decay rate of individual Stark states was calculated as the weighted decay rate of the case (d) basis states which contribute to the Stark state

$$\Gamma_{i,\ \text{Stark}}=\Sigma_\alpha|A_{i\alpha}|^2\Gamma_{\alpha,\text{case }(d)}. \tag{14}$$

As discussed in the introduction, this decay rate is determined mostly by contributions from low-l states. The lifetime of the individual Stark states is obtained as $\tau_i=(h/2\pi\Gamma_i)$.

With the near transform-limited pulsed dye laser ($\Delta\omega_{\text{laser}}\approx0.005\ \text{cm}^{-1}$) a number of Stark states are excited simultaneously. These Stark states subsequently decay according to their individual decay rates. The measured pulsed field ionization spectrum after a time delay t is calculated as

$$S(\omega_{\text{laser}},t)=\Sigma_i|A_{i\alpha_0}|^2\ \exp[-(\omega_i-\omega_{\text{laser}})^2/\Delta\omega_{\text{laser}}{}^2] \ast\exp(-t/\tau_i). \tag{15}$$

The interpretation of Eq. (15) is that the signal at a given laser frequency ω_{laser} is given as a sum over contributions from all Stark states, with the magnitude of each contribution depending on (i) the amplitude $A_{i\alpha_0}$ of the doorway state $|\alpha_0\rangle_{\text{case }(d)}$ in $|i\rangle_{\text{Stark}}$, (ii) the detuning between the laser and $|i\rangle_{\text{Stark}}$ (the spectrum of the laser pulse is assumed to be Gaussian), and (iii) the lifetime τ_i of $|i\rangle_{\text{Stark}}$. The onset of efficient mixing of the doorway state with the Stark manifold occurs near an electric field strength where the halfwidth of the Stark manifold is approximately equal to the zero-field energy difference between the doorway state $|\alpha_0\rangle_{\text{case }(d)}$ and the high-l manifold, or

$$(3/2)Fn^2\approx\mu/n^3. \tag{16}$$

In a hydrogenic Stark manifold the energy spacing between adjacent Stark states is equal to $3Fn$, suggesting that the average number of Stark states that the laser will excite near the onset for mixing of the doorway state to the high-l manifold is given by

$$N_{\text{laser}}\approx\Delta\omega_{\text{laser}}/3Fn\approx\Delta\omega_{\text{laser}}n^4/2\mu. \tag{17}$$

Under the conditions of the experiments reported in Refs. 11(a) and 11(b) we are in a regime where $N_{\text{laser}}\gg1$.[37] The lifetime enhancement of the f orbital ($\mu\approx0.01$) was experimentally studied near $n=65$, where $N_{\text{laser}}\approx20$. Likewise, for the p orbital ($\mu_{\text{reduced}}\approx-0.29$) the lifetime enhancement was studied near $n=115$, where $N_{\text{laser}}\approx7$. In reality, the number of states within the laser bandwidth is even higher, since the state density in the Stark manifold is increased as a result of the rotational structure of the NO^+ core. It follows that the decays which are experimentally measured do not represent the decay of a single Stark state, but rather the decay of a superposition of Stark states. Since the decay rates are in general not the same for these individual Stark states, the excited population of Rydberg states will undergo a multiexponential decay.

As mentioned, an effective decay time was determined experimentally by fitting the pulsed field ionization decay curves which were measured at peaks in the excitation spectrum to a sum of a single-exponential decay term and a constant term. To make contact with the experiment a similar procedure is now followed for the theoretical calculations. First a peak position ω_{peak} in the pulsed field ionization spectrum was determined by determining a maximum in $S(\omega_{\text{laser}},t=0)$ in the vicinity of the zero-field energy of the doorway state. A theoretical decay time was then determined by comparing the calculated multiexponential decay to a single exponential after a delay time Δt, which was defined as the time at which the calculated signal has dropped to $(1/e)$ of its initial value. If the decay was single-exponential then the decay time τ could be obtained at this point as

$$\tau=-S(\omega_{\text{peak}},\Delta t)/[dS(\omega_{\text{peak}},t)/dt]_{t=\Delta t}. \tag{18}$$

Therefore, we adopt this expression to extract an effective decay time for the multiexponential decay of the superposition of Stark states as well. Using Eq. (18) a single decay time is determined which is representative of the overall shape of the multiexponential decay. Contributions from small fractions of states which decay either very rapidly or very slow compared to the average decay time are deemphasized, which is desirable, since the same happens in an experiment. An expression similar to Eq. (18) has been used before in the literature to characterize multiexponential decays associated with decay processes in polyatomic molecules.[38] We return to this point in our discussion of the lifetime enhancement of the $np(N^+=0)$ series.

IV. SPECTROSCOPIC INFORMATION ON NO

In Table I a summary is given of the spectroscopic information on NO which was used as input to the calcula-

TABLE I. Spectroscopic information on NO used in the calculations.

Quantum defects		
$\mu_{s\sigma}=0.210$ (Ref. 22)[a]		
$\mu_{p\sigma}=0.7038$[b]	$\mu_{p\pi}=0.7410$[b]	
$\mu_{d\sigma}=-0.050$ (Ref. 22)[a]	$\mu_{d\pi}=-0.053$ (Ref. 22)	$\mu_{d\delta}=0.089$ (Ref. 22)
Decay rates		
$\Gamma(s)=500$ cm^{-1} (Ref. 11)	$\Gamma(f)=43$ cm^{-1} (Refs. 11 and 14)	
$\Gamma(p)=1610$ cm^{-1} (Refs. 11 and 14)	$\Gamma_{\text{eff}}(l>3)=4$ cm^{-1} [c]	
$\Gamma(d)=1000$ cm^{-1} (Ref. 14)		
Rotational constant		
$B_{\text{rot}}=1.9842$ cm^{-1} (Ref. 11)		

[a]The $s\sigma/d\sigma$ mixing angle is $-39.7°$ (Ref. 22).
[b]This work (see the text).
[c]This work (see the text).

tions. For the s- and d-orbitals the case (b) quantum defects and the $s\sigma/d\sigma$ mixing angle derived in the MQDT analysis of Fredin *et al.* were used.[21,22] Hund's case (b) p-orbital quantum defects were derived from two of our experimentally observed Rydberg series.[11(b)] Starting from the $A\ ^2\Sigma^+(N_A=0,\ J_A=1/2)$ level, a Rydberg series converging on $N^+=0$ was observed with a quantum defect of 0.7286. Furthermore, starting from the $A\ ^2\Sigma^+(N_A=1,\ J_A=3/2)$ level, a Rydberg series converging on $N^+=1$ was observed with a quantum defect of 0.7038. According to the frame transformation [Eq. (2)] the case (b) and case (d) quantum defects relevant to these configurations are related as[39]

$$\mu(N^+=0,l=1,N=1)=\mu_{p\sigma}/3+2\mu_{p\pi}/3,$$
$$\mu(N^+=1,l=1,N=0)=\mu_{p\sigma}. \tag{19}$$

Using these expressions the values for $\mu_{p\sigma}$ and $\mu_{p\pi}$ given in Table I are obtained. These values are in reasonable agreement with the values of Miescher *et al.*[40] who quoted values of 0.68 and 0.74 for $\mu_{p\sigma}$ and $\mu_{p\pi}$, respectively. As discussed in the theory section, for $l\geqslant 3$ the quantum defects were calculated according to the long range force model, using the parameters determined by Jungen and Miescher.[28]

Decay rates for $l=0-3$ were taken from the paper by Bixon and Jortner,[14] who in turn determined these parameters for $l=1$ and 3 from the experimentally observed lifetimes of the $np(N^+=0)$ and $nf(N^+=2)$ series prior to dc electric field induced lifetime enhancement.[11(a),11(b)] In similar fashion they obtained decay widths for $l=0$ and 2 by considering the measured lifetimes of the $np(N^+=0)$ series after a dc field has enhanced the lifetime.[11(a),11(b)] Information on the decay rates for $l\geqslant 4$ is very scarce. Fujii and Morita recently estimated that the predissociation lifetime of $55g(N^+=0)$ and $55g(N^+=12)$ Rydberg states is on the order of 1 μs (suggesting $\Gamma_0\approx 0.85$ cm^{-1}), however the authors discuss that experimentally it is not clear whether this decay represents the decay of the ng component itself or of the ng component mixed with the nearby high-l manifold.[41] In order to obtain the correct lifetime enhancement factor for the

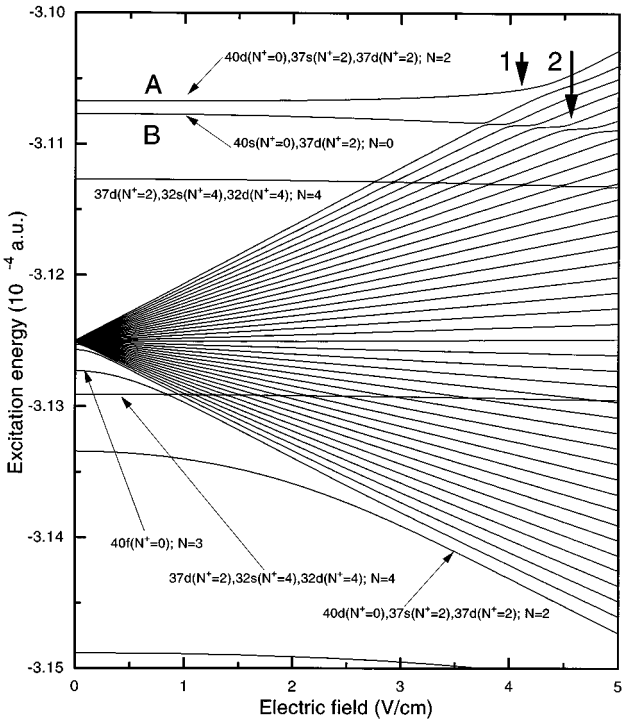

FIG. 4. Calculated Stark map in the vicinity of $n=40$ $(N^+=0)$ showing the energies of a number of penetrating orbitals $l=0-2$ $(N^+=0-4)$ and nonpenetrating orbitals $l\geqslant 3$ $(N^+=0)$ as a function of the existing dc electric field.

$nf(N^+=2)$ series (see below) it was necessary in our calculations to use an effective decay width of 4 cm^{-1} for all case (d) states with $l\geqslant 4$. We acknowledge that this value is certainly higher than would be expected for $l\geqslant 4$, which likely indicates that near the onset for lifetime enhancement our calculations underestimate the admixture of low-l $(l=0-2)$ components.

Finally, the rotational constant which was used in the calculations was obtained from the difference in the experimentally observed convergence limits for the $np(N^+=0)$ and $nf(N^+=2)$ Rydberg series.[11(a),11(b)]

V. RESULTS

To illustrate some of the aspects which determine the dc electric field dependence of the lifetimes of the high-n Rydberg states of NO, a Stark map is shown in Fig. 4. This map shows the existing energy levels in the vicinity of $n=40$ $(N^+=0)$ as a function of the strength of the dc electric field. To obtain this Stark map, a calculation was carried out which included penetrating orbits $l=0-2$ with rotational angular momentum $N^+=0-4$ and nonpenetrating orbitals $l\geqslant 3$ with $N^+=0$. To obtain converged results for the composition of the Stark states, nonpenetrating orbitals with $N^+=2$ and 4 need to be included as well, however in the current example these states are left out for illustrative purposes.

At zero-field energy levels in agreement with the MQDT calculation of Fredin *et al.*[21] are found (see Fig. 3). The low-l orbitals appear at energies which differ by μ/n^3 from

the central energy of the hydrogenic Stark manifold ($\mu=0$). As the dc electric field is turned on, the nearly degenerate high-l states form a linear hydrogenic Stark manifold with a total width equal to $3Fn^2$ and a level spacing of $3Fn$. Upon further increase of the field, low-l orbitals merge into this manifold. The field strength which is required for the mixing of a low-l state with the Stark manifold depends linearly on the magnitude of the quantum defect [Eq. (16)]. The f orbital has a very small quantum defect ($\mu_{40f}=0.0149$) and therefore, requires a dc field of only $\sim$0.5 V/cm. For the other low-l orbitals ($l=0-2$) the quantum defects, and thus the required electric field strengths, are larger.

The quantum defect and the principal quantum number are however not the only parameters which determine at which electric field strength the mixing of a low-l state with the Stark manifold occurs. The mixing of angular momentum states by the electric field is sequential ($\Delta l=\pm 1$), i.e., merging with the Stark manifold starts at the largest values of the orbital angular momentum. This can be illustrated by looking at the evolution of the two curves which are labeled A and B near the top of Fig. 4. These curves correspond to mixtures of $[d(N^+=0),s(N^+=2),d(N^+=2);\ N=2]$ and $[s(N^+=0),d(N^+=2);\ N=0]$, respectively, and are close in energy at zero field. Since the Stark manifold in Fig. 4 is a manifold with an $N^+=0$ core rotational state, the field only mixes states with the manifold to the extent that they contain case (d) states with $N^+=0$ character. State A in our example contains $d(N^+=0)$ character, whereas state B contains $s(N^+=0)$ character. As discussed above, the $f(N^+=0)$ orbital merges into the Stark manifold at about 0.5 V/cm. Consequently, state A [containing $d(N^+=0)$] readily merges into the Stark manifold when the electric field is strong enough for the edge of the Stark manifold to approach the field-free energy of state A, as indicated by arrow 1 in the top right corner of Fig. 4. State B [containing $s(N^+=0)$] does not merge into the manifold until after the $p(N^+=0)$ orbital has done so. The $p(N^+=0)$ orbital has a larger quantum defect ($\mu_{\text{reduced}}\approx -0.29$) and does not mix with the states of the Stark manifold until the electric field reaches a strength of $\sim$10 V/cm. Therefore, at the field strengths shown in Fig. 4, state B does not mix with the states of the Stark manifold, but rather, has a number of avoided crossings with the states of the Stark manifold (see arrow 2 in Fig. 4). Figure 4 shows a number of similar avoided crossings for other states corresponding to mixtures $[d(N^+=2),s(N^+=4),d(N^+=4);\ N=4]$.

A. Lifetime enhancement of $nf(N^+=2)$

Calculations of the lifetimes of nf Rydberg states converging on $N^+=2$ were carried out for $n=25-83$ using the parameters listed in Table I. In each calculation, two energy ranges were defined centered around $E(n)=-1/2n^2$. All states with $l=3\rightarrow(n-1)$ converging on even rotational states $N^+=0-4$ were included within an energy range range $\langle E(n)-(1/4)n^{-3},E(n)+(1/4)n^{-3}\rangle$, whereas for $l=0-2$ all states converging on $N^+=0-4$ in the range $\langle E(n)-5n^{-3},E(n)+5n^{-3}\rangle$ were included. Inclusion of low angular momentum states over a wide range of excitation energies was necessary in these calculations due to the strong perturbations (i.e., fast interseries coupling) which already occur among these states at zero field. We recall that in our model the high-l states are only coupled through interactions which result from the presence of the electric field.

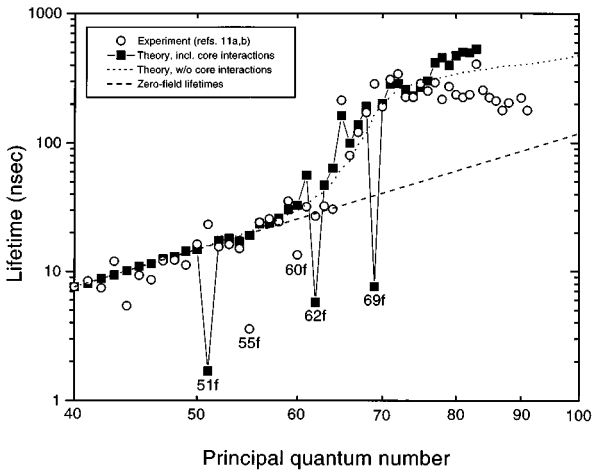

FIG. 5. Calculated (■) and experimental (○) lifetimes of the $nf(N^+=2)$ Rydberg series. The calculations were performed for a dc electric field strength of 40 mV/cm. The dashed line shows the natural (zero field) lifetime of the unperturbed $nf(N^+=2)$ levels. The dotted line represents the result of a calculation in which the matrix elements representing core interactions (H_{core} and H_{sd}) were suppressed.

The results of the calculations are shown in Fig. 5, where a comparison is presented between the calculations and our published experimental results.[11(a),11(b)] The calculations were performed for an electric field strength of 40 mV/cm, which is somewhat higher than the 25 mV/cm value which we inferred experimentally [from extrapolation of the n^{-5} dependence of the critical field strengths for lifetime enhancement of the $np(N^+=0)$ series]. Most likely this discrepancy is due to uncertainties in the minimum residual field in the experimental apparatus, whose source and vector properties are ill-defined. We note that in their calculations[14] Bixon and Jortner also required a field strength of about 40 mV/cm.

In Fig. 5 the lifetimes stay close to their zero-field values (dashed line) until about $n=65$, where both in the experimental and in the theoretical data over a narrow range of states an approximately eightfold lifetime enhancement is observed. As discussed in Sec. IV, in order to reproduce this experimental lifetime enhancement factor an effective decay rate $\Gamma_{\text{effective}}(l\geqslant 4)=4\ \text{cm}^{-1}$ was introduced. Following the rapid increase of the lifetime near $n=65$ the increase slows down. This is due to admixture of low-l contributions to the Stark manifold.

While the calculations reproduce the main features in the experimental data, there are some important differences as well. A number of isolated points stand out where either the experimental data or the theoretical data show minima in the lifetimes. For example, in the experimental data the lifetime of the $55f(N^+=2)N=1$ orbital is measured to be only 3.5 ns, whereas the lifetimes of nearby levels are $\sim$20–25 ns.

Similarly, the lifetime of the $60f(N^+=2)N=1$ is measured to be 13 ns, whereas nearby levels display lifetimes of $\sim$35 ns. The experimental minima in the lifetimes of the $55f$ and $60f$ orbitals are not reproduced in our calculations. Instead, the calculations predict the occurrence of different minima in the lifetimes, for the $51f$, the $62f$, and the $69f$ states. These minima are caused by near-resonances at zero field between the f series and mixed ns/nd states. At zero-field the $51f(N^+=2)N=1$ orbital is nearly degenerate with a mixed state containing $60s(N^+=0)N=0$ and $51d(N^+=2)N=0$, the $62f(N^+=2)N=1$ orbital is nearly degenerate with a mixed state containing $81s(N^+=0)N=0$ and $62d(N^+=2)N=0$, and, finally, the $69f(N^+=2)N=1$ is nearly degenerate with a mixed state containing $99s(N^+=0)N=0$ and $69d(N^+=2)N=0$. The coupling by the electric field mixes the f orbitals with these rapidly decaying s and d components even before the mixing of the f orbital with the high-l manifold sets in. Thus, the observation of these short lifetimes is a manifestation of the role of $H_{\rm core}$ and H_{sd}, and of the interplay between electric field effects and coupling between Rydberg orbitals induced by short range interactions. If these matrix elements describing the short range core interactions are removed, the calculation reduces to pure Hund's case (d), where the quantum defects of the low-l states become independent of n, and where the mixing between different orbitals induced by the electric field follows simple scaling laws. This calculation is shown as the dotted line in Fig. 5. By contrast, as a result of the core interactions described by $H_{\rm core}$ and H_{sd}, the low-l states do not reach the Hund's case (d) limit in our calculation even at the high n values under consideration here. As a function of n the low-l states shift irregularly and some of the states become almost degenerate with members of the $nf(N^+=2)N=1$ series, allowing for facile coupling by the electric field.

The location of the (near-)degeneracies between members of the $nf(N^+=2)$ Rydberg series and ns/nd Rydberg states (with appropriate N^+ and N) depends sensitively on the choice of the spectroscopic input data for the NO molecule. Small changes in the quantum defects lead to a disappearance of some of the near-degeneracies discussed above and the appearance of new ones. Therefore, it seems plausible that the experimentally observed short lifetimes of the $55f(N^+=2)$ and $60f(N^+=2)$ orbitals may be explained by interactions between these states and nearby mixed ns/nd states. This hypothesis could be tested by extending the measurements of Fredin *et al.*[21] of the zero-field Rydberg excitation spectrum of ns and nd orbital Rydberg series towards higher principal quantum numbers.

B. Lifetime enhancement of $np(N^+=0)$

Calculations on the dc electric field induced lifetime enhancement of the $np(N^+=0)$ Rydberg series were carried out for $n=40-150$. As in the calculations reported in the previous section, a central energy was defined as $E=-1/2n^2$. Once more, for orbitals with $l=0-2$ all states converging on even rotational states $N^+=0-4$ were included in a range $\langle E(n)-5n^{-3},E(n)+5n^{-3}\rangle$. Unlike the previous calculation however, nonpenetrating orbitals with $l=3\rightarrow(n-1)$ were included in a wider energy range $\langle E(n)-(5/4)n^{-3},E(n)+(5/4)n^{-3}\rangle$, i.e., both the $N^+=0$ Stark manifold nearest to the $np(N^+=0)$ doorway state and the next $N^+=0$ Stark manifold on either side were included in the calculation (as well as, naturally, $N^+=2$ and $N^+=4$ Stark manifolds within the prescribed energy range).

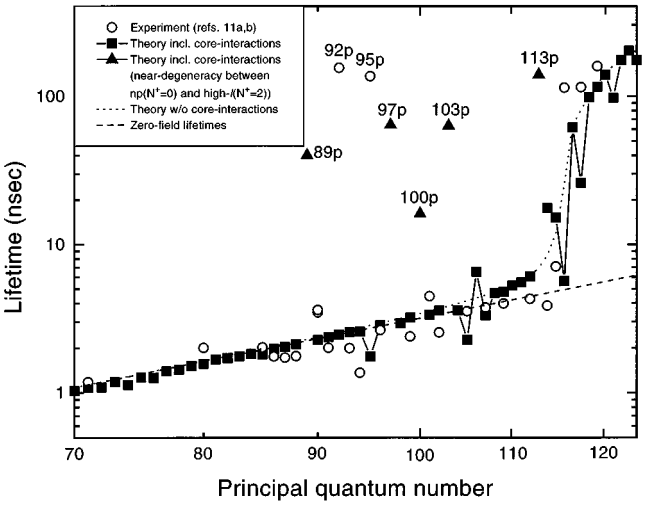

FIG. 6. Calculated (■) and experimental (○) lifetimes of the $np(N^+=0)$ Rydberg series. The calculations were performed for a dc electric field strength of 70 mV/cm. The dashed line shows the natural (zero field) lifetime of the unperturbed $np(N^+=0)$ levels. The dotted line represents the result of a calculation using a field of 60 mV/cm in which the matrix elements representing core interactions ($H_{\rm core}$ and H_{sd}) were suppressed. Special points labeled (▲) are results of the calculations including core interactions where the lifetimes of the $np(N^+=0)$ series members are enhanced via coupling to the nearly degenerate high-l manifold of a Rydberg series converging on $N^+=2$.

The results are shown in Fig. 6, where the experimental results are compared to a calculation for a dc electric field of 70 mV/cm. This is the field strength which is required to achieve the onset of the lifetime enhancement at the principal quantum number where the enhancement was observed experimentally ($n=115$). As in the case of the nf series, this electric field strength differs from the experimentally inferred electric field strength. We note that a field of 70 mV/cm also exceeds by about 30% the field that would be anticipated on the basis of Eq. (16), due to the fact that the $np(N^+=0)$ energy levels curve away from the Stark manifold as the electric field increases (see Fig. 4), resulting in a larger absolute value of the reduced quantum defect at the onset of efficient mixing.

The calculation reproduces the very sharp onset of the lifetime enhancement near $n=115$ quite successfully. Whereas for $115p(N^+=0)$ a decay time of 5.6 ns is calculated, the decay time of the $116p(N^+=0)$ state increases one order of magnitude to 63 ns. However, the sharp onset of the lifetime enhancement is only partly a molecular effect. Figure 6 also shows (dotted line) that the onset of the lifetime enhancement can be reproduced almost equally well in a calculation in which the matrix elements H_{sd} and $H_{\rm core}$,

which describe core mixing of the penetrating orbitals $l=0-2$, are removed, albeit using a slightly smaller electric field of 60 mV/cm. The onset of the lifetime enhancement in the vicinity of $n=115$ is not quite as sharp in this calculation, but it is hard to decide whether the calculation including H_{sd} and H_{core} leads to a better reproduction of the experimental results. The differences between the calculations with and without H_{sd} and H_{core} do attest, however, to the important role played by short range interactions in the NO molecule. The quality of the experimental results on the one hand and our ability to *quantitatively* predict the short range perturbations on the other do not allow us to definitively pinpoint the effects of short range interactions in the experimental results. Nevertheless, a comparison of the calculations with and without the short range interactions illustrates that short range interactions are very important in the region where the lifetime enhancement sets in.

The onsets of the lifetime enhancement which are shown experimentally and theoretically in Fig. 6 are significantly sharper than those calculated by Bixon and Jortner.[14] This is primarily due to the definition of the decay time [Eq. (18)] which describes the experimental and theoretical multiexponential decay of the superposition of (Stark) states which are excited within the bandwidth of the excitation laser. Bixon and Jortner extracted an effective decay time τ which was defined by $S(\omega_{\mathrm{peak}},\tau)/S(\omega_{\mathrm{peak}},t=0)=(1/e)$. In other words, the decay time was defined as the delay time at which the population of Rydberg states has decayed to a fraction $(1/e)$ of its initial value. According to this definition the transition from unmixed to mixed states takes place over a relatively broad region of $\Delta n\approx 20$. Experimentally, it is very difficult to measure states which decay on a time scale which is comparable or shorter than the duration of the excitation laser pulse ($\sim$7 ns). Consequently, our experiment is relatively insensitive to the presence of (Stark) states in the superposition with lifetimes $\leqslant$5 ns. Similarly, since the pulsed field ionization signal is measured superimposed on a background due to ionization of Rydberg states by the excitation laser, our experiment is relatively insensitive to the presence of a small fraction ($<$10%) of states in the superposition, which decay on a time scale which exceeds the average decay time in the superposition substantially. Rather, the experiment emphasizes the decay time of those states which represent the biggest fraction of the Rydberg population and thereby set the time scale for the decay of the major portion of Rydberg molecules. This is why Eq. (18) was used to extract an effective decay time from the calculations. The lifetime calculated using Eq. (18) represents the time constant for a single-exponential decay that would look identical to our multiexponential decay in the region where the Rydberg population has dropped to $(1/e)$ of its initial value.

While some of the main features of the lifetime spectrum are reproduced by a calculation which ignores H_{sd} and H_{core}, we do find further evidence of core interactions in our calculations. In Fig. 6, the $89p$, $97p$, $100p$, $103p$, and $113p$ states (indicated by ▲) show lifetime enhancements well before the threshold at $n=115$. These lifetime enhancements are due to a near-resonance between the $np(N^+=0)$ series and the high-l $(N^+=2)$ manifold. The $np(N^+=0)$ series can couple to this manifold mediated by mixed $(s(N^+=0),d(N^+=2);\ N=0)$ and $(d(N^+=0),s(N^+=2),d(N^+=2);\ N=2)$ states. Unfortunately, the premature lifetime enhancement of these $np(N^+=0)$ series members could not be verified experimentally in Refs. 11(a) and 11(b), since the n values where $np(N^+=0)$ is nearly degenerate with a $(N^+=2)$ Stark manifold naturally coincide with the n values where the $np(N^+=0)$ and $nf(N^+=2)$ series are badly overlapped. Therefore, no measurements were performed for the $np(N^+=0)$ series at these values of the principal quantum number.

With reference to Fig. 6, we reiterate that our calculations do not reproduce the premature lifetime enhancement of the $92p(N^+=0)$ and $95p(N^+=0)$ Rydberg states, since the long range Rydberg electron–core dipole interaction was not included.[14]

VI. SUMMARY

In this paper, results have been presented of calculations on the lifetime enhancement of high principal quantum number Rydberg states of the NO molecule in a small dc electric field. Calculations were carried out for the lifetime enhancement of $nf(N^+=2)$ and $np(N^+=0)$ Rydberg series and compared to experimental results which were reported in an earlier paper.[11(a),11(b)] Guided by an earlier MQDT analysis by Fredin *et al.* concerning the field-free energy levels of the NO molecule,[21] a perturbative approach was used, emphasizing the role of short range interactions among core-penetrating orbitals with orbital angular momentum $l=0-2$. These short range interactions lead to substantial mixing of low-l Rydberg states with different core rotational states, as well as mixing between s- and d-orbital Rydberg series. Our calculations complement the work by Bixon and Jortner,[14] who considered the possible role of Rydberg electron–core dipole interactions and arrived at the conclusion that this interaction is negligible, except for a few isolated instances where near-degeneracies occur.

Three results of the calculations are emphasized. First of all, these calculations provide a testing ground for the applicability of perturbative methods to the spectroscopy of high-n Rydberg states, as was demonstrated by a comparison of our results at zero field to MQDT results calculated by Fredin *et al.* Our calculations show that it is possible to satisfactorily represent short range interactions in a perturbative method. This opens the way to theoretical calculations involving both short range and long range interactions simultaneously.

Secondly, with these calculations an explanation has been provided for the experimentally observed lifetime enhancements of the $nf(N^+=2)$ and $np(N^+=0)$ Rydberg series, including the experimentally observed discontinuity in the measured lifetimes of the $np(N^+=0)$ Rydberg series near $n=115$, which had defied explanation before. In our calculations a sharp onset of the lifetime enhancement of the $np(N^+=0)$ is observed, which is partly due to the influence

of short range interactions. In the region where the lifetime-enhancement occurs, significant perturbations occur among the low-l Rydberg states as a result of short range interactions, which lead to appreciable differences between lifetimes which are calculated with or without these interactions. It needs to be stressed, however, that for the most part the rapid onset of the lifetime enhancement arises from our definition of the effective decay time of a superposition of Stark states, which differs from the definition used earlier by Bixon and Jortner.[14]

Thirdly, we note that the short range interactions further manifest themselves in a number of isolated perturbations for both the $nf(N^+=2)$ and $np(N^+=0)$ Rydberg series. In the case of the $nf(N^+=2)$ series several instances were identified, where a small electric field was sufficient to mix the nf series with a nearby member of the perturbed $s(N^+=2)$ or $d(N^+=2)$ Rydberg series, leading to a reduction in the lifetime. In the case of the $np(N^+=0)$ Rydberg series a number of states displayed a premature lifetime enhancement owing to coupling to nearly degenerate $N^+=2$ high-l manifolds, mediated by mixed $s/d(N^+=0,2)$ states which arise as a result of $s\sigma/d\sigma$ mixing.

ACKNOWLEDGMENTS

I especially would like to thank Joshua Jortner and Mordechai Bixon for their encouragement and for making Ref. 14 available prior to publication. I further would like to acknowledge Bill Chupka (Yale), Jim Watson, Klaus Huber and Albert Stolow (Ottawa), Stephen Ross (New Brunswick), Christian Jungen, Helene Lefebre-Brion, and Dolores Gauyacq (Orsay), Frederic Merkt (Zürich), Leonid Baranov, and Raphy Levine (Jerusalem), and Francoise Remacle (Liege), with all of whom I enjoyed important and stimulating discussions. Finally, I would like to thank Yuan Lee (Taipei), in whose laboratories at Berkeley the experiments discussed in this paper were originally carried out, and Steven Stolte (Amsterdam) for carefully reading the manuscript prior to publication. This research was supported by the Royal Dutch Academy of Sciences (KNAW).

[1] K. Müller-Dethlefs and E. W. Schlag, Annu. Rev. Phys. Chem. **42**, 109 (1991).
[2] K. Müller-Dethlefs, E. W. Schlag, E. R. Grant, K. Wang, and B. V. McKoy, Adv Chem Phys. **XC**, 1 (1995).
[3] G. Reiser, W. Habenicht, K. Müller-Dethlefs, and E. W. Schlag, Chem. Phys. Lett. **152**, 119 (1988).
[4] (a) D. Bahatt, U. Even, and R. D. Levine, J. Chem. Phys. **98**, 1744 (1993); (b) U. Even, M. Ben-nun, and R. D. Levine, Chem. Phys. Lett. **210**, 416 (1993); (c) F. Remacle and R. D. Levine, Phys. Lett. A **173**, 284 (1993); (d) U. Even, R. D. Levine, and R. Bersohn, J. Phys. Chem. **98**, 3472 (1994); (e) E. Rabani, L. Ya. Baronov, R. D. Levine, and U. Even, Chem. Phys. Lett. **221**, 473 (1994); (f) E. Rabani, R. D. Levine, and U. Even, J. Phys. Chem. **98**, 8834 (1994); (g) E. Rabani, R. D. Levine, A. Mühlpfordt, and U. Even, J. Chem. Phys. **102**, 1619 (1995); (h) A. Mühlpfordt, U. Even, E. Rabani, and R. D. Levine, Phys. Rev. A **51**, 3922 (1995); (i) F. Remacle and R. D. Levine, J. Chem. Phys. **104**, 1399 (1996); (j) E. Rabani and R. D. Levine, *ibid*. **104**, 1937 (1996).
[5] (a) C. Alt, W. G. Scherzer, H. L. Selzle, and E. W. Schlag, Chem. Phys. Lett. **224**, 366 (1994); (b) W. G. Scherzer, H. L. Selzle, and E. W. Schlag, Z. Naturforsch. Teil A **48**, 1256 (1994); (c) W. G. Scherzer, H. L. Selzle, E. W. Schlag, and R. D. Levine, Phys. Rev. Lett. **72**, 1435 (1994); (d) C. E. Alt, W. G. Scherzer, H. L. Selzle, E. W. Schlag, L. Ya. Baronov, and R. D. Levine, J. Phys. Chem. **99**, 1660 (1995); (e) C. Alt, W. G. Scherzer, H. L. Selzle, and E. W. Schlag, Chem. Phys. Lett. **240**, 457 (1995); (f) Ber. Bunsenges. Phys. Chem. **99**, 332 (1995).
[6] (a) W. A. Chupka, J. Chem. Phys. **98**, 4520 (1993); (b) **99**, 5800 (1993).
[7] (a) F. Merkt, H. H. Fielding, and T. P. Softley, Chem. Phys. Lett. **202**, 153 (1993); (b) F. Merkt, J. Chem. Phys. **100**, 2623 (1994); (c) F. Merkt and R. N. Zare, *ibid*. **101**, 3495 (1994); (d) F. Merkt, H. Xu, and R. N. Zare, *ibid*. **104**, 950 (1996).
[8] (a) J. Jortner and M. Bixon, J. Chem. Phys. **102**, 5636 (1995); (b) M. Bixon and J. Jortner, J. Phys. Chem. **99**, 7466 (1995); (c) J. Chem. Phys. **103**, 4431 (1995).
[9] X. Zhang, J. M. Smith, and J. L. Knee, J. Chem. Phys. **99**, 3133 (1993).
[10] S. T. Pratt, J. Chem. Phys. **98**, 9241 (1993).
[11] (a) M. J. J. Vrakking and Y. T. Lee, Phys. Rev. A **51**, R894 (1995); (b) J. Chem. Phys. **102**, 8818 (1995); (c) **102**, 8833 (1995); (d) M. J. J. Vrakking, I. Fischer, D. M. Villeneuve, and A. Stolow, *ibid*. **103**, 4538 (1995).
[12] E. Lee, D. Farrelly, and T. Uzer, Chem. Phys. Lett. **231**, 241 (1994).
[13] C. Bordas, P. F. Brevet, M. Broyer, J. Chevaleyre, P. Labastie, and J. P. Perrot, Phys. Rev. Lett. **60**, 917 (1988).
[14] M. Bixon and J. Jortner, J. Chem. Phys. **105**, 1363 (1996).
[15] U. Fano, Phys. Rev. A **2**, 353 (1970).
[16] C. H. Greene and Ch. Jungen, Adv. Atom. Mol. Phys. **21**, 51 (1985).
[17] (a) D. A. Harmin, Phys. Rev. A **24**, 2491 (1981); (b) **26**, 2656 (1982); (c) **30**, 2413 (1984).
[18] K. Sakimoto, J. Phys. B: At. Mol. Opt. Phys. **22**, 2727 (1989).
[19] P. F. Brevet, Ch. Bordas, M. Broyer, G. Jalbert, and P. Labastie, J. Phys. II France **1**, 875 (1991).
[20] H. H. Fielding and T. P. Softley, Phys. Rev. A **49**, 969 (1994).
[21] S. Fredin, D. Gauyacq, M. Horani, C. Jungen, and G. Lefevre, Mol. Phys. **60**, 825 (1987).
[22] D. Gauyacq, A. L. Roche, M. Seaver, S. D. Colson, and W. A. Chupka, Mol. Phys. **71**, 1311 (1990).
[23] G. Herzberg and Ch. Jungen, J. Mol. Spectrosc. **41**, 425 (1972).
[24] A. Giusti-Suzor and Ch. Jungen, J. Chem. Phys. **80**, 986 (1984).
[25] W. E. Ernst, T. P. Softley, and R. N. Zare, Phys. Rev. A **37**, 4172 (1988).
[26] C. Bordas and H. Helm, Phys. Rev. A **45**, 387 (1992).
[27] A. D. Buckingham, Discuss Faraday Soc. **41**, 232 (1965).
[28] Ch. Jungen and E. Miescher, Can. J. Phys. **47**, 1769 (1969).
[29] Ch. Jungen, J. Chem. Phys. **53**, 4168 (1970).
[30] K. Qin, M. Bistransin, and W. L. Glab, Phys. Rev. A **47**, 4154 (1993).
[31] M. J. J. Vrakking (unpublished).
[32] K. T. Lu, Phys. Rev. A **4**, 579 (1971).
[33] W. Weizel, *Bandenspektren* (Akademische Verlagsgesellschaft, Leipzig, 1931).
[34] E. U. Condon and G. H. Shortley, *The Theory of Atomic Spectra* (Cambridge University Press, Cambridge, 1964).
[35] A. R. Edmonds, *Angular Momentum in Quantum Mechanics* (Princeton University Press, New Jersey, 1957).
[36] A. R. Edmonds, J. Picart, N. Tran Minh, and R. Pullen, J. Phys. B **12**, 2781 (1979).
[37] Experiments are currently under preparation to measure lifetimes in Stark manifolds in the intermediate principal quantum number regime where $N_{\text{laser}} \leqslant 1$.
[38] See, for example, F. Remacle, M. Desouter-Lecomte, and J. C. Lorquet, J. Chem. Phys. **91**, 4155 (1989).
[39] An alternative assignment for the second series as $N^+=1$, $l=1$, $N=1$ leads to unphysical values of $\mu_{p\sigma}$ and $\mu_{p\pi}$ of 0.481 and 0.853, respectively.
[40] E. Miescher, Y. T. Lee, and P. Gürtler, J. Chem. Phys. **68**, 2753 (1978).
[41] A. Fujii and N. Morita, J. Chem. Phys. **103**, 6029 (1995).